

Cite this: *CrystEngComm*, 2011, **13**, 3064

www.rsc.org/crystengcomm

PAPER

Fabrication of nanoporous material from a hydrophobic peptide†

Sibaprasad Maity, Poulami Jana and Debasish Haldar**

Received 7th October 2010, Accepted 8th February 2011

DOI: 10.1039/c0ce00701c

A pentapeptide containing hydrophobic residues self-assembles to form nonporous materials in solid state. The X-ray crystallography reveals that there is no pore in the crystal and the peptide exhibits supramolecular helical architecture prompted by the formation of intra- and intermolecular hydrogen bonds. But the phase-selective gelation of the peptide from xylene–water leads to the formation of nanoporous material with different internal diameter. The field emission scanning electron micrographs (FE-SEM) show that the average pore size is in the range of 20 to 50 nm. Moreover, the nanoporous xerogel can efficiently adsorb I₂ and remove organic dyes from wastewater.

Introduction

Fabrication of nanoporous materials is a highly interesting area of recent research due to their potential application in gas storage, sensors, ion exchange, purifications, catalysis and separation.¹ In particular, the nanoporous materials have a strong propensity to interact with atoms, ions, molecules and adsorb on their nanometre sized pore space and in the large interior surfaces.² Up to now, several effective strategies, such as emulsion processes, surface-protected etching, supramolecular self-assembly, as well as the replication method, have been developed to prepare organic microporous (below 2 nm), mesoporous (2–50 nm) and macroporous (>50 nm) materials containing predictable porous topologies.³ But it has proved difficult to form organic polymer networks with perfectly controlled pore dimensions.⁴

Many industries including textile, leather, paper, plastic, printing, foods and cosmetics, use large quantities of dyes and produce toxic wastewater with residual dyes. This toxic color interferes with the penetration of sunlight into water, gas solubility in water and also pollutes the aquatic ecological system. So, the removal of toxic dyes from wastewater is highly important. Recently organic–inorganic hybrid gels,⁵ activated charcoal, clay, porous silica, different polymers⁶ and such types of different scaffolds are used for removing dyes from wastewater.⁷

Recently, we have reported the formation of polydisperse nanopores by the self-assembly of a β -turn forming tripeptide as an associating sub-unit that also acts as *in situ* reducing agent and

synthesized hexagonal gold nanoparticles.⁸ Herein, we present the conversion of a nonporous peptide into a nanoporous material in the presence of water. From X-ray crystallography, there is no pore in the crystal and the peptide **1** exhibits supramolecular helical architecture prompted by the formation of intra- and intermolecular hydrogen bonds. Water mediated gelation of the peptide from xylene leads to the formation of nanoporous material with average pore size in the range of 20 to 50 nm. Moreover, the nanoporous xerogel can efficiently adsorb I₂ and remove organic dyes from wastewater.

Results and discussion

Synthesis and solid state analysis

The pentapeptide Boc-Leu(1)-Val(2)-Aib(3)-Phe(4)-Aib(5)-OMe (**1**) consisting of hydrophobic amino acid residues, has been synthesized by conventional solution-phase methodology and purified, characterized and studied. There are two conformationally constrained Aib residues to increase the helical nature of the peptide backbone and enhance the crystallinity.⁹ Solid-state FT-IR spectroscopy was performed to study the secondary structure of the peptide **1**. The region 1800–1500 cm⁻¹ is important for the stretching band of amide I, bending peak of amide II and hydrogen bonded urethane groups.¹⁰ Another informative frequency range is 3500–3200 cm⁻¹, corresponding to the N–H stretching vibrations of the peptide.¹⁰ An intense band at 3319 cm⁻¹ indicates the presence of strongly hydrogen-bonded NH groups. No band has been observed at around 3400 cm⁻¹, indicating that all NH groups are involved in intra- and intermolecular hydrogen bonding.¹¹ The amide I band at 1654 cm⁻¹ and amide II band at 1528 cm⁻¹ suggest that the peptide adopts helical structure in solid state (Fig. 1).¹² The helical structure of the peptide **1** was further studied by single crystal X-ray diffraction. The colorless orthorhombic crystal of the peptide **1** was obtained from methanol solution by slow evaporation.¹³ The ORTEP diagram of peptide **1** with the atomic

Department of Chemical Sciences, Indian Institute of Science Education and Research, Kolkata, Mohanpur, West Bengal, 741252, India. E-mail: deba_h76@yahoo.com; deba_h76@iiserkol.ac.in; Fax: +91 34 73 279131; Tel: +91 34 73 279130

† Electronic supplementary information (ESI) available: Synthesis and characterization of peptides, ¹H NMR and ¹³C NMR (Fig. S1–S4 and S5–S13). CCDC reference number 772430. For ESI and crystallographic data in CIF or other electronic format see DOI: 10.1039/c0ce00701c

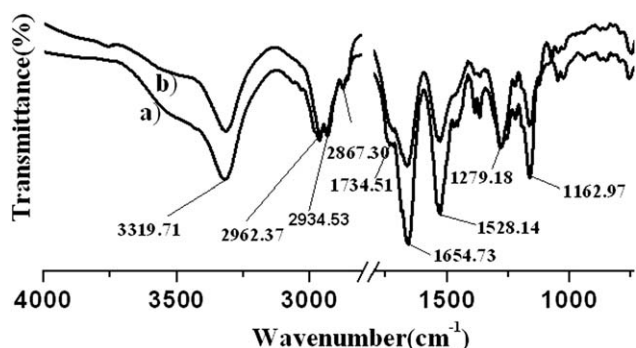


Fig. 1 FT-IR spectra of pentapeptide **1** in (a) solid and (b) xerogel from xylene–water.

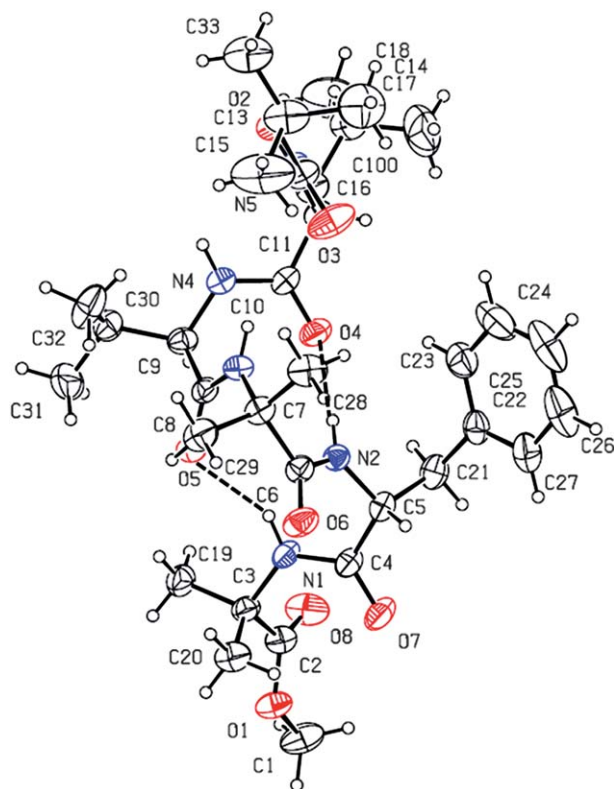


Fig. 2 The ORTEP diagram of pentapeptide **1** showing the atomic numbering scheme. Ellipsoids are drawn at the 30% probability level. Intramolecular hydrogen bonds are shown as dotted line.

Table 1 Selected backbone torsion angles (°) for peptide **1**

C12–N5–C11–C10	66.2 ϕ_1	N3–C7–C6–N2	33.2 ψ_3
N5–C11–C10–N4	33.4 ψ_1	C6–N2–C5–C4	75.5 ϕ_4
C10–N4–C9–C8	66.5 ϕ_2	N2–C5–C4–N1	15.9 ψ_4
N4–C9–C8–N3	22.6 ψ_2	C4–N1–C3–C2	–56.8 ϕ_5
C6–C7–N3–C8	53.3 ϕ_3	N1–C3–C2–O1	142.5 ψ_5

numbering scheme is shown in Fig. 2. The solid state conformation of peptide **1** shows that there are two consecutive β -turn structures where Aib(2) occupies the $i + 2^{\text{nd}}$ position of the first turn and $i + 1^{\text{st}}$ position for the second turn.¹⁴ Most of the backbone torsion angles (Table 1) of peptide **1** are in the left

handed helical region of the Ramachandran diagram [except ϕ_5 (-56.8°) and ψ_5 (142.5°) values of Aib(5)]. From Fig. 2 there are two intramolecular hydrogen bonds N1–H1 \cdots O5 and N2–H2 \cdots O4 resulting in a helical conformation for individual peptide molecules in the solid state. The individual helical sub-units of peptide **1** are themselves regularly inter-linked through an intermolecular hydrogen bonding interaction N5–H5b \cdots O7 and thereby form a supramolecular left handed helix along the crystallographic a direction (Fig. 3).¹⁵ Moreover, in higher order packing, the supramolecular helical columns are interdigitated by non-covalent interactions and formed a supramolecular helical bundle according to the crystallographic c axis (Fig. 4).¹⁶ The space filling presentation of higher order crystal packing (ESI, Fig. S1 \dagger) shows that there are no pores in the crystal. The hydrogen bonding parameters of peptide **1** are listed in Table 2.

Phase-selective gelation and thermal behaviour

The phase-selective gelation from a given mixture of solvents is an interesting task due to its many applications.¹⁷ The peptide **1** forms a clear solution at elevated temperatures in aromatic solvents and microcrystals are precipitated out of the solution on cooling. In the present study, peptide **1** was found to be suitable for selective gelation from an organic solvent/water mixture. In a typical procedure, 1 mL of xylene and 1 mL of water were shaken in a sample tube and 80 mg of the peptide **1** was added. The tube was heated to dissolve the compound in the organic

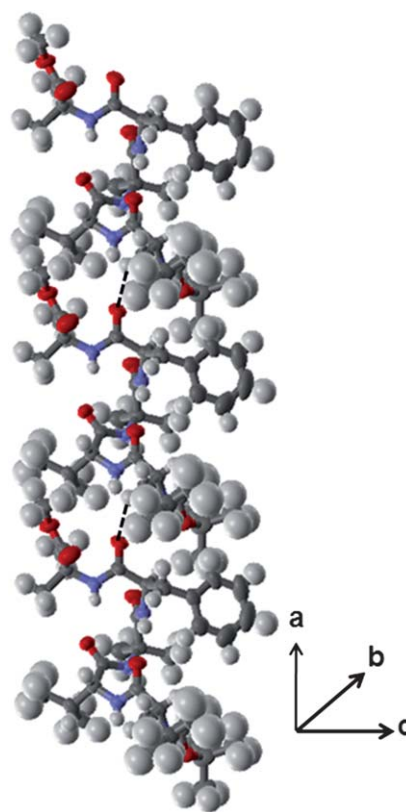


Fig. 3 Supramolecular helix from self-assembly of peptide **1** along the crystallographic a direction. Intermolecular hydrogen bonds are shown as dotted line.

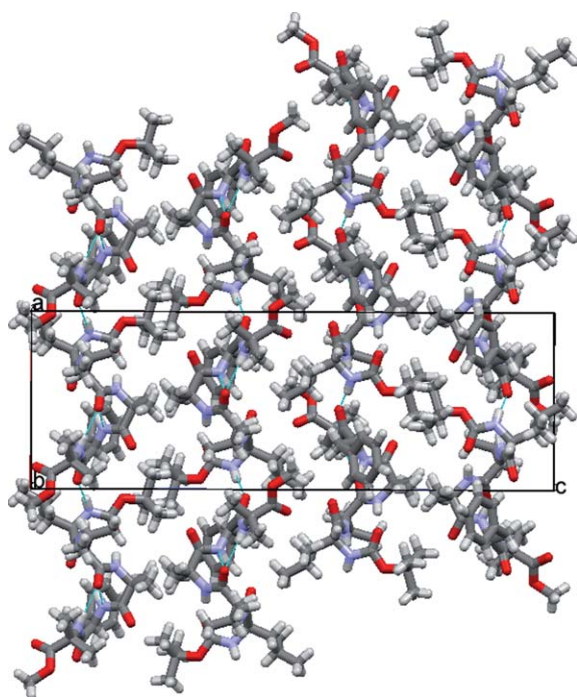


Fig. 4 Packing diagram of peptide **1** showing supramolecular helical columns which are further self-assembled to form helical bundle.

Table 2 Hydrogen bonding parameters of peptide **1**

D–H...A	H...A/Å	D...A/Å	D–H...A/°
N1–H1...O5	2.27	3.03	148
N2–H2...O4	2.5	3.33	164
N5–H5 ^a ...O7	2.24	2.90	133

^a Symmetry equivalent $-1+x, y, z$.

phase (xylene) and then it was shaken vigorously to ensure homogeneous dispersion. After cooling at room temperature the organic phase gelled entrapping the water inside the tube (Fig. 5). The gelation was confirmed by the inverted test tube method. The gels are white, opaque and stable for months at room temperature. The gel is thermoreversible. The sol–gel transition temperature (T_{gel}) of the peptide **1** in xylene increases

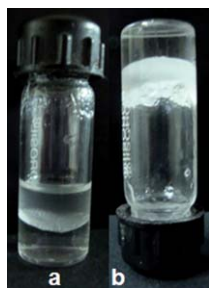


Fig. 5 Selective organic liquid gelation over water. (a) Clear solution of peptide **1** in xylene over water after heating. (b) The opaque gel after cooling. The aqueous phase (top) is trapped by the gel.

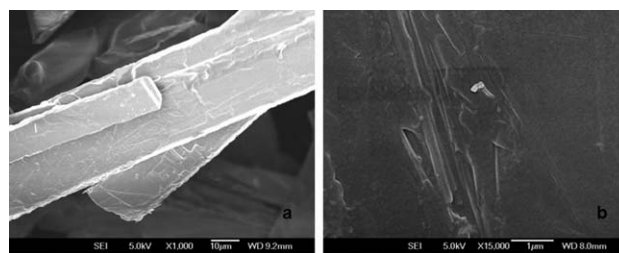


Fig. 6 FE-SEM images of peptide **1** microcrystal from xylene solution (a) and the surface of microcrystal (b) exhibits no pores.

with increasing gelator concentration (ESI, Fig. S2[†]), a feature generally observed for low molecular weight (LMW) gels.¹⁸

Morphology and characterization

To obtain insight into the morphology of the reported peptide in gel state, field-emission scanning electron microscopic (FE-SEM) measurements were carried out.¹⁹ For FE-SEM experiments, peptide **1** solution in xylene was drop cast on a microscopic glass slide and dried under vacuum and studied. Fig. 6 exhibits the microcrystals obtained from the xylene solution. Moreover, there are no pores visible on the surface of the microcrystal.

For FE-SEM studies, xerogel of peptide **1** from xylene–water was placed on a microscopic glass slide and then further dried under vacuum for two days. Fig. 7 depicts the FE-SEM image of the peptide xerogel. In Fig. 7, the micrograph shows the porous nanostructure morphology in their self-assembled state and the pores are polydisperse in nature with different diameters. Average pore size is 20–50 nm from solid state. The selected area electron diffraction (SAED) experiment (transmission electron microscopy) of xerogel (from xylene–water) exhibits the many ordered scattering spots (Fig. 8).

Though it is apparent from the FT-IR spectrum (Fig. 1) that both the solid compound (crystal) and xerogel (from xylene–water) have almost identical structure. Fig. 9 shows the wide angle X-ray scattering (WAXS) patterns of solid powder as synthesized (a), xerogel from xylene–water (b) and powder pattern from single crystal X-ray (c). From the three spectra it is clear that there is a significant change in position and intensity of the major peaks for as-synthesized solid material, xerogel and crystal. In fact, sharp reflections are observed in the 20–25° 2θ

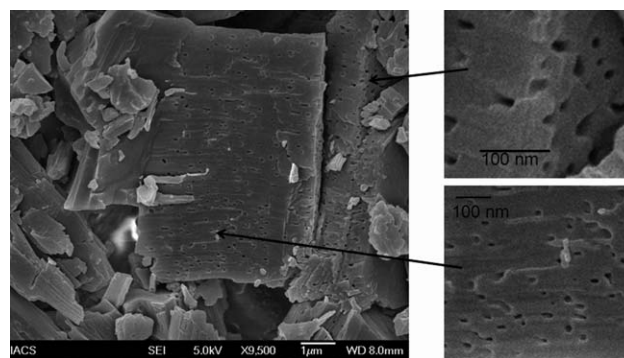


Fig. 7 Field emission scanning electron microscopic image of peptide **1** xerogel showing nanoporous morphology in the solid state.

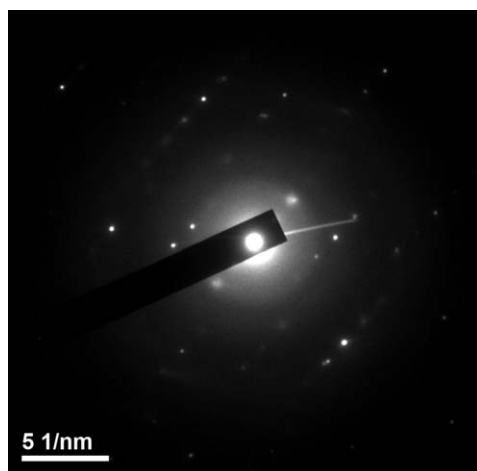


Fig. 8 SAED (TEM) pattern of peptide 1 xerogel from xylene-water.

range for the as-synthesized materials and crystal whereas only a very broad feature was observed in the xerogels (Table 3). Also in the 15–20° 2θ range, there are more sharp reflections in xerogels than in crystal.

Adsorption in nanopores

In order to examine the pores in xerogel, I_2 absorption studies have been performed. The peptide 1 crystals and nanoporous xerogel were exposed to I_2 vapors.²⁰ Exposure of the sample was carried out in a closed chamber for 24 h. It was observed that the nanoporous xerogel of peptide 1 turned dark brown (Fig. 10), whereas the crystals turned yellowish brown. The nature of the absorption was verified by crushing the xerogel of peptide 1 after iodine exposure. The dark brown color inside the nanoporous xerogel indicates uniform absorption of I_2 .

Moreover, we have used nanoporous peptide 1 xerogel obtained from xylene-water as a filter for dye removal. Absorption of dye molecules from their respective aqueous solutions was monitored by UV-visible spectroscopy. 5 mg of nanoporous xerogel were added to 3 mL of 0.001 mM crystal

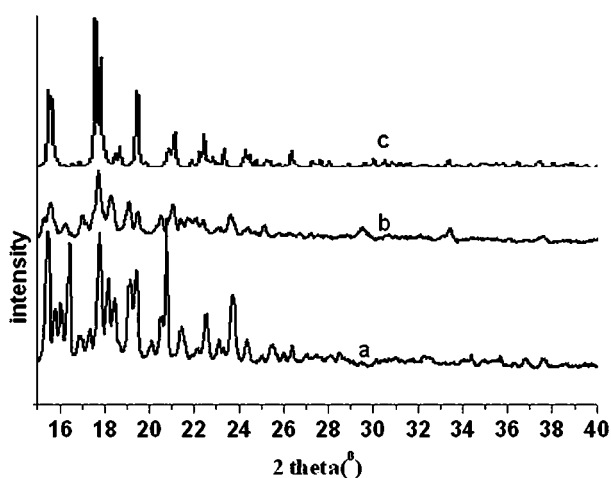


Fig. 9 WAXS spectra of pentapeptide 1 in (a) solid, (b) xerogel from xylene-water and (c) powder pattern from single crystal X-ray.

Table 3 Analysis and comparison of major X-ray peaks obtained from peptide 1 crystal, as synthesized solid powder and xerogel from xylene-water

	d -spacing/Å
Crystal	5.59, 4.98, 4.93, 4.84, 4.53, 4.23, 4.19, 3.95, 3.80, 3.65, 3.38
Solid	5.74, 5.61, 5.53, 5.39, 5.24, 5.10, 4.98, 4.88, 4.80, 4.64, 4.63, 4.56, 4.42, 4.33, 4.27, 4.14, 3.94, 3.85, 3.74, 3.49, 3.37
Xerogel	5.77, 5.68, 5.44, 5.21, 4.99, 4.83, 4.64, 4.55, 4.33, 3.76, 3.63, 3.54



Fig. 10 Pentapeptide 1 (a) crystals and (b) xerogel from xylene-water showing colour change after exposure to I_2 vapours.

violet solution. For Rhodamine 6G, 3 mL of 0.005 mM dye solution was treated with 5 mg of xerogel. The UV-visible spectroscopy shows that the maximum amount of the crystal violet (ESI, Fig. S3†) and Rhodamine 6G (Fig. 11) was absorbed by nanoporous xerogel leaving a nearly clear solution after 24 h. The maximum amount of crystal violet absorbed by xerogel is 7.0 mg g^{-1} and Rhodamine 6G is 4.5 mg g^{-1} .

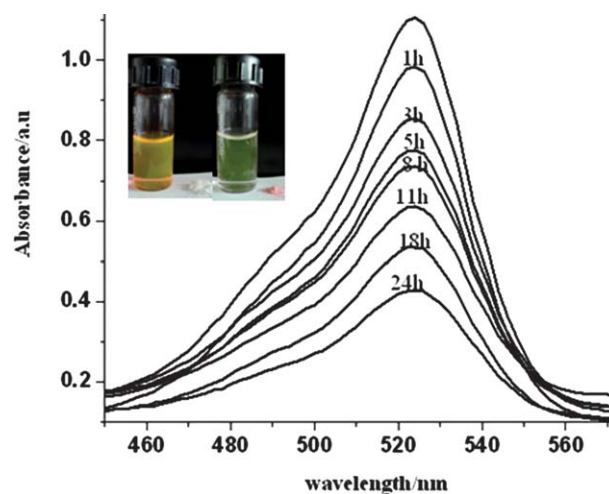


Fig. 11 UV-vis spectra for time dependent absorption of Rhodamine 6G from aqueous solution by the pentapeptide 1 xerogel from xylene-water.

Experimental

General methods and materials

All L-amino acids were purchased from Sigma chemicals. HOBt (1-hydroxybenzotriazole) and DCC (dicyclohexylcarbodiimide) were purchased from SRL.

Peptide synthesis

The peptides were synthesized by conventional solution-phase methodology using racemization free fragment condensation strategy.²¹ The Boc group was used for N-terminal protection and the C-terminus was protected as a methyl ester. Couplings were mediated by dicyclohexylcarbodiimide/1-hydroxybenzotriazole (DCC/HOBt). Methyl ester deprotection was performed by the saponification method. All the intermediates were characterized by 500 MHz ¹H and ¹³C NMR and FT-IR spectroscopy. The final compound was fully characterized by 500 MHz ¹H NMR spectroscopy, ¹³C NMR spectroscopy, FT-IR spectroscopy and mass spectrometry. The peptide **1** was characterized by X-ray crystallography.

(a) Boc-Leu-OH (2). A solution of L-Leucine (2.62 g, 20 mmol) in a mixture of dioxane (40 mL), water (20 mL) and 1 M NaOH (20 mL) was stirred and cooled in an ice-water bath. Di-*tert*-butylpyrocarbonate (4.8 g, 22 mmol) was added and stirring was continued at room temperature for 6 h. Then the solution was concentrated in vacuum to about 20–30 mL, cooled in an ice-water bath, covered with a layer of ethyl acetate (about 50 mL) and acidified with a dilute solution of KHSO₄ to pH 2–3 (Congo red). The aqueous phase was extracted with ethyl acetate and this operation was done repeatedly. The ethyl acetate extracts were pooled, washed with water and dried over anhydrous Na₂SO₄ and evaporated under vacuum. The pure material was obtained as a waxy solid.

Yield: 3.81 g (16.5 mmol, 82.5%).

¹H NMR (500 MHz, DMSO-*d*₆, δ ppm): 12.36 [br, 1H, –COOH], 7.03–7.02 [d, 1H, *J* = 8 Hz, Leu(1) NH], 3.91–3.87 [m, 1H, Leu(1) C α H], 1.64–1.61 [m, 2H, Leu(1) C β H], 1.51–1.47 [m, 1H, Leu(1) C γ H], 1.36 [s, 9H, Boc CH₃], 0.87–0.83 [m, 6H, Leu(1) C δ H]. ¹³C NMR (125 MHz, DMSO-*d*₆, δ ppm): 174.73, 155.64, 77.76, 66.41, 51.81, 28.24, 24.38, 22.92, 21.24. FT-IR (KBr): 3462, 3355, 3311, 2983, 2968, 2934, 2877, 2525, 1727, 1699, 1675, 1533, 1456, 1419, 1385, 1368, 1296, 1197, 1172, 1087, 1048, 1018 cm⁻¹.

(b) Boc-Leu-Val-OMe (3). 3.698 g (16 mmol) of Boc-Leu-OH was dissolved in 25 mL dry DCM in an ice-water bath. H-Val-OMe was isolated from 5.365 g (32 mmol) of the corresponding methyl ester hydrochloride by neutralization, subsequent extraction with ethyl acetate and the ethyl acetate extract was concentrated to 10 mL. It was then added to the reaction mixture, followed immediately by 3.3 g (16 mmol) of dicyclohexylcarbodiimide (DCC) and 2.45 g (16 mmol) of HOBt. The reaction mixture was allowed to come to room temperature and stirred for 48 h. DCM was evaporated and the residue was dissolved in ethyl acetate (60 mL) and dicyclohexylurea (DCU) was filtered off. The organic layer was washed with 2 M HCl (3 \times 50 mL), brine (2 \times 50 mL), 1 M sodium carbonate (3 \times 50 mL)

and brine (2 \times 50 mL) and dried over anhydrous sodium sulfate, and evaporated under vacuum to yield Boc-Leu-Val-OMe as a white solid. Purification was done by silica gel column (100–200 mesh size) and ethyl acetate and hexane 1 : 3 as eluent.

Yield: 3.85 g (11.26 mmol, 70.37%); mp: 116 °C.

¹H NMR (500 MHz, CDCl₃, δ ppm): 6.61–6.60 [d, 1H, *J* = 7.5 Hz, Val(2) NH], 4.91–4.89 [d, 1H, *J* = 8 Hz, Leu(1) NH], 4.53–4.51 [m, 1H, Leu(1) C α H], 4.11–4.10 [m, 1H, Val(2) C α H], 3.72 [s, 3H, OCH₃], 2.18–2.13 [m, 1H, Val(2) C β H], 1.69–1.63 [m, 2H, Leu(1) C β H], 1.48–1.47 [m, 1H, Leu(1) C γ H], 1.45 [s, 9H, Boc CH₃], 0.94–0.88 [m, 12H, Leu(1) C δ and Val(2) C γ]. ¹³C NMR (125 MHz, CDCl₃, δ ppm) 172.09, 171.56, 155.74, 79.87, 59.36, 57.00, 52.10, 36.90, 31.20, 28.26, 24.77, 18.89, 17.69, 15.48, 11.31. FT-IR (KBr): 3330, 3082, 2966, 2874, 2873, 1750, 1687, 1661, 1557, 1458, 1438, 1393, 1367, 1290, 1242, 1208, 1180, 1048, 1025, 925, 877, 785, 767, 647 cm⁻¹.

Anal calcd for C₁₇H₃₂N₂O₅ (344.45): C, 59.28; H, 9.36; N, 8.13. Found: C, 59.25; H, 9.40; N, 8.22%.

(c) Boc-Leu-Val-OH (4). To 3.82 g (11.17 mmol) of Boc-Leu-Val-OMe, 25 mL MeOH and 2 M 15 mL NaOH were added and the progress of saponification was monitored by thin layer chromatography (TLC). The reaction mixture was stirred. After 10 h, methanol was removed under vacuum; the residue was dissolved in 50 mL of water, and washed with diethyl ether (2 \times 50 mL). Then the pH of the aqueous layer was adjusted to 2 using 1 M HCl and it was extracted with ethyl acetate (3 \times 50 mL). The extracts were pooled, dried over anhydrous sodium sulfate, and evaporated under vacuum to obtain the compound as a waxy solid.

Yield: 3.56 g (10.77 mmol, 96.41%).

¹H NMR (DMSO-*d*₆, 500 MHz, δ ppm): 12.67 [br, 1H, COOH], 7.71–7.69 [d, 1H, *J* = 8 Hz, Val(2) NH], 7.00–6.99 [d, 1H, *J* = 8.5 Hz, Leu(1) NH], 4.17–4.14 [m, 1H, Leu(1) C α H], 4.03–3.99 [m, 1H, Val(2) C α H], 2.06–2.02 [m, 1H, Val(2) C β H], 1.63–1.57 [m, 2H, Leu(1) C β H], 1.45–1.40 [m, 1H, Leu(1) C γ H], 1.38 [s, 9H, Boc CH₃], 0.88–0.87 [m, 12H, Leu(1) C δ H and Val(2) C γ H]. ¹³C NMR (DMSO-*d*₆, 125 MHz, δ ppm): 172.82, 172.61, 155.25, 78.01, 56.72, 52.84, 40.56, 30.14, 28.14, 24.21, 22.96, 21.53, 18.97, 17.80. FT-IR (KBr): 3321, 2969, 2935, 2880, 1716, 1684, 1656, 1538, 1466, 1419, 1392, 1367, 1292, 1245, 1172, 1045, 1020, 929, 868, 782, 650 cm⁻¹.

Anal calcd for C₁₆H₃₀N₂O₅ (330.42): C, 58.16; H, 9.15; N, 8.48. Found: C, 58.14; H, 9.18; N, 8.50%.

(d) Boc-Leu-Val-Aib-OMe (5). 3.56 g (10.774 mmol) of Boc-Leu-Val-OH was dissolved in 15 mL dry DCM in an ice-water bath. H-Aib-OMe 3.38 g (22 mmol) was isolated from corresponding methyl ester hydrochloride by neutralization, subsequent extraction with ethyl acetate and concentrated to 7 mL. Then it was added to the reaction mixture, followed immediately by 2.22 g (10.77 mmol) dicyclohexylcarbodiimide (DCC) and 1.64 g (10.77 mmol) HOBt. The reaction mixture was allowed to come to room temperature and stirred for 72 h. The residue was taken in 30 mL ethyl acetate and dicyclohexylurea (DCU) was filtered off. The organic layer was washed with 2 M HCl (3 \times 50 mL), brine (2 \times 50 mL), then 1 M sodium carbonate (3 \times 30 mL) and brine (2 \times 30 mL) and dried over anhydrous sodium sulfate and evaporated under vacuum to yield the

tripeptide as a white solid. Purification was done by silica gel column (100–200 mesh size) and ethyl acetate and hexane (1 : 2) as eluent.

Yield: 3.04 g (7.077 mmol, 65.68%); mp: 114 °C.

¹H NMR (CDCl₃, 500 MHz, δ ppm): 6.66 [s, 1H, Aib(3) NH], 6.60–6.58 [d, 1H, J = 8.5 Hz, Val(2) NH], 4.87 [b, 1H, Leu(1) NH], 4.19–4.16 [m, 1H, Leu(1) C α H], 4.07–4.06 [m, 1H, Val(2) C α H], 3.71 [s, 3H, –OCH₃], 2.27–2.21 [m, 1H, Val(2) C β H], 1.65–1.65 [m, 3H, Leu(1) C β H & C γ H], 1.52 [s, 6H, Aib(3) CH₃], 1.44 [s, 9H, Boc CH₃], 0.953–0.919 [m, 12H, Leu(1) C δ H and Val(2) C γ H]. ¹³C NMR (CDCl₃, 125 MHz, δ ppm): 174.61, 172.55, 170.04, 155.74, 79.87, 58.27, 56.31, 52.41, 40.76, 31.20, 28.26, 24.77, 19.10, 17.47, 15.48. FT-IR (KBr): 3328, 2959, 2932, 2870, 1749, 1690, 1648, 1542, 1388, 1367, 1290, 1243, 1172, 1045, 1024 cm⁻¹.

Anal calcd for C₂₁H₃₉N₃O₆ (429.55): C, 58.72; H, 9.16; N, 9.78. Found: C, 58.75; H, 9.18; N, 9.76%.

(e) Boc-Leu-Val-Aib-OH (6). To 3.0 g (7.0 mmol) of compound **4**, 25 mL MeOH and 2 M 15 mL NaOH were added and the progress of saponification was monitored by thin layer chromatography (TLC). The reaction mixture was stirred. After 10 h, methanol was removed under vacuum; the residue was dissolved in 50 mL of water, and washed with diethyl ether (2 \times 50 mL). Then the pH of the aqueous layer was adjusted to 2 using 1 M HCl and it was extracted with ethyl acetate (3 \times 50 mL). The extracts were pooled, dried over anhydrous sodium sulfate, and evaporated under vacuum to obtain the compound as a waxy solid.

Yield: 2.35 g (5.65 mmol, 79.83%).

¹H NMR (DMSO-*d*₆, 500 MHz, δ ppm): 12.19 [s, 1H, –COOH], 8.18 [s, 1H, Aib(3) NH], 7.47–7.45 [d, 1H, J = 9 Hz, Val(2) NH], 7.13–7.12 [d, 1H, J = 8.5 Hz, Leu(1) NH], 4.19–4.16 [m, 1H, C α H Leu(1)], 3.95–3.92 [m, 1H, Val(2) C α H], 1.94–1.90 [m, 1H, Val(2) C β H], 1.59–1.56 [m, 2H, Leu(1) C β H], 1.43–1.40 [m, 1H, Leu(1) C γ H], 1.40 [s, 6H, Aib(3) CH₃], 1.31 [s, 9H, Boc CH₃], 0.87–0.83 [m, 12H, Leu(1) C δ H and Val(2) C γ H]. ¹³C NMR (DMSO-*d*₆, 125 MHz, δ ppm) 175.25, 169.88, 155.84, 78.12, 56.66, 54.67, 53.15, 31.33, 28.13, 24.95, 24.54, 24.26, 22.89, 21.58, 18.96, 17.73. FT-IR (KBr): 3298, 2963, 2936, 2870, 1718, 1654, 1535, 1387, 1367, 1281, 1248, 1170, 1046, 1021, 937, 875, 781, 610 cm⁻¹.

Anal calcd for C₂₀H₃₇N₃O₆ (415.52): C, 57.81; H, 8.98; N, 10.11. Found: C, 57.91; H, 9.04; N, 10.0%.

(f) Boc-Leu-Val-Aib-Phe-OMe (7). 2.32 g (5.6 mmol) of compound **5** was dissolved in 25 mL dry DCM in an ice-water bath. H-Phe-OMe was isolated from 2.41 g (11.2 mmol) of the corresponding methyl ester hydrochloride by neutralization, subsequent extraction with ethyl acetate and the ethyl acetate extract was concentrated to 10 mL and then added to the reaction mixture, followed immediately by 1.155 g (5.6 mmol) dicyclohexylcarbodiimide (DCC) and 0.857 g (5.6 mmol) of HOBt. The reaction mixture was allowed to come to room temperature and stirred for 72 h. DCM was evaporated and the residue was dissolved in ethyl acetate (60 mL) and dicyclohexylurea (DCU) was filtered off. The organic layer was washed with 2 M HCl (3 \times 50 mL), brine (2 \times 50 mL), 1 M sodium carbonate (3 \times 50 mL) and brine (2 \times 50 mL) and dried over anhydrous sodium sulfate,

and evaporated under vacuum to yield compound **7** as a white solid. Purification was done by silica gel column (100–200 mesh size) and ethyl acetate and hexane (1 : 3) as eluent.

Yield: 1.51 g (2.61 mmol, 46.19%).

¹H NMR (500 MHz, CDCl₃, δ ppm): 7.27–7.20 [m, 5H, aromatic ring protons], 7.16–7.14 [d, 1H, J = 7 Hz, Phe(4) NH], 6.74 [s, 1H, Aib(3) NH], 6.59–6.57 [d, 1H, J = 7.5 Hz, Val(2) NH], 4.88–4.87 [d, 1H, J = 8 Hz, Leu(1) NH], 4.80–4.76 [m, 1H, Phe(4) C α H], 4.10–4.07 [m, 1H, Leu(1) C α H], 4.05–4.03 [m, 1H, Val(2) C α H], 3.69 [s, 3H, –OCH₃], 3.18–3.05 [m, 2H, Phe(4) C β H], 2.31–2.21 [m, 1H, Val(2) C β H], 1.71–1.65 [m, 2H, Leu(1) C β H], 1.63 [s, 3H, Aib(3) CH₃], 1.48 [s, 3H, Aib(3) CH₃], 1.44 [s, 9H, Boc CH₃], 1.41 [m, 1H, Leu(1) C γ H], 0.95–0.88 [m, 12H, Leu(1) C δ H Val(2) C γ H]. ¹³C NMR (125 MHz, CDCl₃, δ ppm): 173.88, 172.95, 171.92, 170.34, 155.86, 136.75, 129.33, 128.37, 126.86, 80.67, 59.14, 57.30, 55.83, 53.57, 52.20, 40.41, 37.82, 29.77, 28.23, 25.51, 24.80, 24.70, 22.93, 21.77, 19.32, 17.41. FT-IR (KBr): 3332, 2961, 2927, 2872, 2346, 1747, 1651, 1524, 1455, 1391, 1366, 1245, 1172, 1118, 1046, 1024 cm⁻¹.

Anal calcd for C₃₀H₄₈N₄O₇ (576.72): C, 62.48; H, 8.39; N, 9.71. Found: C, 62.52; H, 8.45; N, 9.76%.

(g) Boc-Leu-Val-Aib-Phe-OH (8). To 1.5 g (2.61 mmol) of compound **7**, 25 mL MeOH and 2 M 15 mL NaOH were added and the progress of saponification was monitored by thin layer chromatography (TLC). The reaction mixture was stirred. After 10 h, methanol was removed under vacuum; the residue was dissolved in 50 mL of water, and washed with diethyl ether (2 \times 50 mL). Then the pH of the aqueous layer was adjusted to 2 using 1 M HCl and it was extracted with ethyl acetate (3 \times 50 mL). The extracts were pooled, dried over anhydrous sodium sulfate, and evaporated under vacuum to obtain the compound as a waxy solid.

Yield: 1.46 g (2.59 mmol, 99.2%).

¹H NMR (DMSO-*d*₆, 500 MHz, δ ppm): 12.75 [br, 1H, –COOH], 7.98 [s, 1H, Aib(3) NH], 7.61–7.59 [d, 1H, J = 8 Hz, Phe(4) NH], 7.39–7.38 [d, 1H, J = 8 Hz, Val(2) NH], 7.26–7.15 [m, 5H aromatic ring protons], 7.05–7.03 [d, 1H, J = 8.5 Hz, Leu(1) NH], 4.40–4.35 [m, 1H, Phe(4) C α H], 4.10–4.07 [m, 1H, Leu(1) C α H], 3.96–3.95 [m, 1H, Val(2) C α H], 3.01–2.90 [m, 2H, Phe(4) C β H], 1.95–1.89 [m, 1H, Val(2) C β H], 1.55–1.53 [m, 2H, Leu(1) C β H], 1.39–1.36 [m, 1H, Leu(1) C γ H], 1.34 [s, 9H, Boc CH₃], 1.32 [s, 6H, Aib(3) CH₃], 0.81–0.78 [m, 12H, Leu(1) C δ H, Val(2) C γ H]. ¹³C NMR (DMSO-*d*₆, 125 MHz, δ ppm): 129.18, 128.07, 126.36, 78.04, 56.00, 53.46, 40.09, 36.77, 28.12, 25.00, 24.20, 23.12, 21.79, 19.13, 17.89. FT-IR (KBr): 3422, 2959, 2928, 2855, 1657, 1532, 1385, 1261, 1169, 1169, 1047, 1024, 800 cm⁻¹.

Anal calcd for C₂₉H₄₆N₄O₇ (562.7): C, 61.90; H, 8.24; N, 9.96. Found: C, 62.00; H, 8.25; N, 9.86%.

(h) Boc-Leu-Val-Aib-Phe-Aib-OMe (1). 1.15 g (2.57 mmol) of compound **7** was dissolved in 25 mL DCM in an ice-water bath. H-Aib-OMe was isolated from 1.38 g (9.0 mmol) of the corresponding methyl ester hydrochloride by neutralization, subsequent extraction with ethyl acetate and the ethyl acetate extract was concentrated to 10 mL. It was then added to the reaction mixture, followed immediately by 0.530 g (2.57 mmol) dicyclohexylcarbodiimide (DCC) and 0.393 g (2.57 mmol) of HOBt. The

reaction mixture was allowed to come to room temperature and stirred for 72 h. DCM was evaporated and the residue was dissolved in ethyl acetate (60 mL) and dicyclohexylurea (DCU) was filtered off. The organic layer was washed with 2 M HCl (3 × 50 mL), brine (2 × 50 mL), 1 M sodium carbonate (3 × 50 mL) and brine (2 × 50 mL) and dried over anhydrous sodium sulfate, and evaporated in a vacuum to yield Boc-Leu-Val-Aib-Phe-Aib-OMe as a white solid. Purification was done by silica gel column (100–200 mesh size) and ethyl acetate and hexane (1 : 3) as eluent.

Yield: 1.19 g (1.80 mmol, 69.49%); mp: 144–145 °C.

¹H NMR (CDCl₃, 500 MHz, δ ppm): 7.39 [s, 1H, Aib(3) NH], 7.19 [s, 1H, Aib(5) NH], 7.15–7.13 [d, 1H, *J* = 7 Hz, Phe(4) NH], 7.29–7.19 [m, 5H, aromatic ring protons], 6.55–6.54 [d, 1H, *J* = 5.5 Hz, Val(2) NH], 4.94 [b, 1H, Leu(1) NH], 4.66–4.62 [m, 1H, Phe(4) CαH], 4.01–3.97 [m, 1H, Leu(1) CαH], 3.92–3.91 [m, 1H, Val(2) CαH], 3.72 [s, 3H, –OCH₃], 3.52–2.88 [m, 2H, Phe(4) CβH], 2.28–2.24 [m, 1H, Val(2) CβH], 1.74–1.71 [m, 2H, Leu(1) CβH], 1.54 [s, 6H, Aib(5) CH₃], 1.50 [s, 3H, Aib(5) CH₃], 1.46 [s, 9H, Boc CH₃], 1.45 [s, 3H, Aib(5) CH₃], 1.27 [m, 1H, Leu(1) CγH], 1.03–0.94 [m, 12H, Leu(1) CδH and Val(2) CγH]. ¹³C NMR (CDCl₃, 125 MHz, δ ppm): 175.17, 174.02, 173.92, 171.03, 170.87, 156.47, 138.38, 129.29, 128.14, 126.22, 81.49, 60.41, 57.16, 55.91, 54.38, 52.20, 40.20, 36.88, 28.92, 28.24, 28.17, 26.72, 25.32, 24.89, 24.67, 23.50, 22.84, 21.63, 19.18, 17.59. FT-IR (KBr): 3320, 2962, 2936, 2874, 1734, 1685, 1654, 1528, 1466, 1458, 1387, 1366, 1279, 1222, 1163, 1048, 1023, 758, 702 cm⁻¹.

Anal calcd for C₃₄H₅₅N₄O₈ (661.83): C, 61.70; H, 8.38; N, 10.58. Found: C, 61.66; H, 8.43; N, 10.62%.

NMR experiments

All NMR studies were carried out on a Bruker AVANCE 500 MHz spectrometer at 278 K. Compound concentrations were in the range 1–10 mM in CDCl₃ and (CD₃)₂SO.

FT-IR spectroscopy

All reported solid-state FT-IR spectra were obtained with a Perkin Elmer Spectrum RX1 spectrophotometer with the KBr disk technique.

Mass spectrometry

Mass spectra were recorded on a Q-ToF Micro YA263 high-resolution (Waters Corporation) mass spectrometer by positive-mode electrospray ionization.

UV-visible spectroscopy

UV-visible absorption spectra were recorded on a UV-visible spectrophotometer (Perkin Elmer).

Phase-selective gelation

80 mg of the peptide **1** was shaken in a sample tube with 1 mL of xylene and 1 mL of water. The tube was heated and shaken vigorously to ensure homogeneous dispersion. The organic phase gelled on cooling.

Field emission scanning electron microscopy

The morphologies of the reported materials were investigated by field emission scanning electron microscope (FE-SEM). For the SEM study, a small amount of the peptide **1** solution in xylene and the gel materials were drop cast on a glass slide and dried and coated with platinum. Then the micrographs were taken in an SEM apparatus (JEOL microscope JSM-6700F).

Transmission electron microscopy

The TEM studies were performed using a small amount of the gel materials on carbon-coated copper grids (300 mesh) by slow evaporation and allowed to dry under vacuum at 30 °C for 2 days. Images were taken both in the transmission mode and diffraction mode. TEM was done by a JEOL JEM 2010 electron microscope.

X-ray crystallography

Single crystal X-ray analysis of peptide **1** was recorded on a Bruker high-resolution X-ray diffractometer instrument.

Wide angle X-ray diffraction study

The WAXS pattern was made on the solid and the xerogel of peptide **1** from xylene–water. The experiment was carried out in a Seifert X-ray diffractometer (C 3000) with a parallel beam optics attachment. The instrument was operated at a 45 kV voltage and 200 mA current and was calibrated with a standard silicon sample. The sample was scanned from 15° to 40° (2θ) at the step scan mode (step size 0.02°, preset time 2 s) and the diffraction pattern was recorded using a scintillation scan detector. The wavelength of the X-ray source is 1.5418 Å (Kα value of Cu).

Conclusions

In conclusion, the conversion of a hydrophobic peptide into a nanoporous material by the presence of water has been discussed. The X-ray crystallography reveals that there is no pore in the crystal and the peptide **1** exhibits supramolecular helical architecture prompted by the formation of intra- and intermolecular hydrogen bonds. Water mediated gelation of the peptide from xylene leads to the formation of nanoporous material with average pore size in the range of 20 to 50 nm. Moreover, the nanoporous xerogel can efficiently absorb I₂ and remove organic dyes from wastewater. These findings presented here may provide useful guidelines for the design of nanomaterials having applications in the fields of absorption, encapsulation of active ingredients, and separation techniques.

Acknowledgements

We acknowledge the DST, New Delhi, India, for financial assistance Project No. (SR/FT/CS-041/2009). S. Maity and P. Jana wishes to acknowledge the C.S.I.R, New Delhi, India for research fellowship. We are thankful to Dr Raju Mandal, Department of Inorganic Chemistry, I.A.C.S., Jadavpur, Kolkata-700032, India, for his assistance in X-ray crystallography data refinement. We gratefully acknowledge the I.A.C.S.,

Jadavpur, Kolkata-700032, India, for using the Mass Spectrometry, X-ray crystallography, TEM and FE-SEM facility.

Notes and references

- (a) M. E. Davis, *Nature*, 2002, **417**, 813–821; (b) J. L. Atwood, L. J. Barbour, A. Jerga and B. L. Schottel, *Science*, 2002, **298**, 1000–1002; (c) G. D. Enright, K. A. Udachin, I. L. Moudrakovski and J. A. Ripmeester, *J. Am. Chem. Soc.*, 2003, **125**, 9896–9897; (d) S. Lim, H. Kim, N. Selvapalam, K. J. Kim, S. J. Cho, G. Seo and K. Kim, *Angew. Chem., Int. Ed.*, 2008, **47**, 3352–3355; (e) K. J. Msayib, D. Book, P. M. Budd, N. Chaukura, K. D. M. Harris, M. Helliwell, S. Tedds, A. Walton, J. E. Warren, M. Xu and N. B. McKeown, *Angew. Chem., Int. Ed.*, 2009, **48**, 3273–3277; (f) A. Stein, *Adv. Mater.*, 2003, **15**, 763–775; (g) J. Fan, C. Yu, J. Lei, Q. Zhang, T. Li, B. Tu, W. Zhou and D. Zhao, *J. Am. Chem. Soc.*, 2005, **127**, 10794; (h) M. M. Conn and J. Rebek, Jr, *Chem. Rev.*, 1997, **97**, 1647–1668; (i) K. D. M. Harris, *Chem. Soc. Rev.*, 1997, **26**, 279–289; (j) V. A. Russell, C. C. Evans, W. Li and M. D. Ward, *Science*, 1997, **276**, 575–579.
- (a) B. D. Chandler, G. D. Enright, K. A. Udachin, S. Pawsey, J. A. Ripmeester, D. T. Cramb and G. K. H. Shimizu, *Nat. Mater.*, 2008, **7**, 229–235; (b) P. K. Thallapally, B. P. McGrail, S. J. Dalgarno, H. T. Schaefer, J. Tian and J. L. Atwood, *Nat. Mater.*, 2008, **7**, 146–150.
- (a) D. Ni, L. Wang, Y. Sun, Z. Guan, S. Yang and K. Zhou, *Angew. Chem., Int. Ed.*, 2010, **49**, 4223–4227; (b) Y. Zhao and L. Jiang, *Adv. Mater.*, 2009, **21**, 3621–3638; (c) G. J. A. A. Soler-Illia, C. Sanchez, B. Lebeau and J. Patarin, *Chem. Rev.*, 2002, **102**, 4093–4138; (d) J. Jang and K. Lee, *Chem. Commun.*, 2002, 1098–1099; (e) Z. Ao, Z. Yang, J. F. Wang, G. Z. Zhang and T. Ngai, *Langmuir*, 2009, **25**, 2572–2574; (f) Q. Zhang, T. R. Zhang, J. P. Ge and Y. D. Yin, *Nano Lett.*, 2008, **8**, 2867–2871; (g) L. J. Zhang and M. X. Wan, *Adv. Funct. Mater.*, 2003, **13**, 815–820.
- P. M. Budd, *Science*, 2007, **316**, 210–211.
- (a) V. Bekiari and P. Lianos, *Chem. Mater.*, 2006, **18**, 4142–4146; (b) E. J. Cho, I. Y. Jeong, S. J. Lee, W. S. Han, J. K. Kang and J. H. Jung, *Tetrahedron Lett.*, 2008, **49**, 1076–1079.
- (a) H. Kasgöz and A. Durmus, *Polym. Adv. Technol.*, 2008, **19**, 838–845; (b) H. Kasgöz, *Polym. Bull.*, 2006, **56**, 517–528.
- (a) T. Polubesova, S. Nir, D. Zakada, O. Rabinovitz, C. Serban, L. Groisman and B. Rubin, *Environ. Sci. Technol.*, 2005, **39**, 2343–2348; (b) A. Sayari, S. Hamoudi and Y. Yang, *Chem. Mater.*, 2005, **17**, 212–216; (c) M. Arkas, D. Tsiourvas and C. M. Paleos, *Chem. Mater.*, 2005, **17**, 3439–3444; (d) S. Ray, A. K. Das and A. Banerjee, *Chem. Mater.*, 2007, **19**, 1633–1639.
- P. Jana, S. Maity and D. Haldar, *CrystEngComm*, 2011, **13**, 973–978.
- (a) D. Haldar, M. G. B. Drew and A. Banerjee, *Tetrahedron*, 2007, **63**, 5561–5566; (b) D. Haldar, M. G. B. Drew and A. Banerjee, *Tetrahedron*, 2006, **62**, 6370–6378.
- (a) C. Toniolo and M. Palumbo, *Biopolymers*, 1977, **16**, 219–224; (b) V. Moretto, M. Crisma, G. M. Bonora, C. Toniolo, H. Balaram and P. Balaram, *Macromolecules*, 1989, **22**, 2939–2944; (c) D. Haldar and A. Banerjee, *Int. J. Pept. Res. Ther.*, 2007, **13**, 439–446.
- (a) G. P. Dado and S. H. Gellman, *J. Am. Chem. Soc.*, 1994, **116**, 1054–1062; (b) D. Haldar and A. Banerjee, *Int. J. Pept. Res. Ther.*, 2006, **12**, 341–348.
- (a) S. E. Blondelle, B. Forood, A. R. Houghten and E. Peraz-Paya, *Biochemistry*, 1997, **36**, 8393–8400; (b) P. I. Haris and D. Chapman, *Biopolymers*, 1995, **37**, 251–263.
- Crystal data for peptide I: C₃₄H₅₅N₅O₈, *M_w* = 661.83, orthorhombic, space group *P*2₁2₁2₁, *a* = 10.974(3), *b* = 11.196(3), *c* = 32.379(9) Å, *U* = 3978 Å³, *Z* = 4, *d_m* = 1.105 Mg m⁻³. Intensity data were collected with MoK α radiation at room temperature using Bruker APEX-2 CCD diffractometer. The crystal was positioned at 70 mm from the Image Plate. 100 frames were measured at 2° intervals with a counting time of 5 min to give 8110 independent reflections. Data were processed using the Bruker SAINT package and the structure solution and refinement procedures were performed using SHELX97.²² The non-hydrogen atoms were refined with anisotropic thermal parameters. The hydrogen atoms were included in geometric positions and given thermal parameters equivalent to 1.2 times those of the atom to which they were attached. The final *R* values were *R*1 0.0474 and *wR*2 0.2078 for 4671 data with *I* > 2 σ (*I*). The largest peak and hole in the final difference Fourier were –0.15 and 0.2 eÅ⁻³. The data have been deposited at the Cambridge Crystallographic Data Center with reference number CCDC 772430.
- D. Haldar, S. K. Maji, M. G. B. Drew, A. Banerjee and A. Banerjee, *Tetrahedron Lett.*, 2002, **43**, 5465–5468.
- A. K. Das, A. Banerjee, M. G. B. Drew, S. Ray, D. Haldar and A. Banerjee, *Tetrahedron*, 2005, **61**, 5027–5036.
- D. Haldar, A. Banerjee, M. G. B. Drew, A. K. Das and A. Banerjee, *Chem. Commun.*, 2003, 1406–1407.
- S. Bhattacharya and Y. K. Ghosh, *Chem. Commun.*, 2001, 185–186.
- K. J. C. V. Bommel, C. V. D. Pol, I. Mujzebelt, A. Friggeri, A. Heeres, A. Meetsma, B. L. Feringa and J. V. Esch, *Angew. Chem., Int. Ed.*, 2004, **43**, 1663–1667.
- B. Adhikari, G. Palui and A. Banerjee, *Soft Matter*, 2009, **5**, 3452–3460.
- L. Rajput, V. V. Chernyshev and K. Biradha, *Chem. Commun.*, 2010, **46**, 6530–6532.
- M. Bodanszky and A. Bodanszky, *The Practice of Peptide Synthesis*, Springer, New York, 1984, pp 1–282.
- G. M. Sheldrick, *SHELX 97*, University of Göttingen, Germany, 1997, 2007, 19, 6290–6296.